ORIGINAL ARTICLE

Electrocorticographic Encoding of Human Gait in the Leg Primary Motor Cortex

Colin M. McCrimmon[1], Po T. Wang[1], Payam Heydari[2], Angelica Nguyen[3], Susan J. Shaw[4,5], Hui Gong[4,5], Luis A. Chui[6], Charles Y. Liu[7,8,9], Zoran Nenadic[1,2] and An H. Do[6]

[1]Department of Biomedical Engineering, University of California Irvine, Irvine, CA, USA, [2]Department of Electrical Engineering and Computer Science, University of California Irvine, Irvine, CA, USA, [3]Electrophysiology Lab, Rancho Los Amigos National Rehabilitation Center, Downey, CA, USA, [4]Department of Neurology, Rancho Los Amigos National Rehabilitation Center, Downey, CA, USA, [5]Department of Neurology, University of Southern California, Los Angeles, CA, USA, [6]Department of Neurology, University of California Irvine, Irvine, CA, USA, [7]Department of Neurosurgery, Rancho Los Amigos National Rehabilitation Center, Downey, CA, USA, [8]Center for Neurorestoration, University of Southern California, Los Angeles, CA, USA and [9]Department of Neurosurgery, University of Southern California, Los Angeles, CA, USA

Address correspondence to Colin M. McCrimmon, Zoran Nenadic, Department of Biomedical Engineering, University of California Irvine, 3120 Natural Sciences II, Irvine, CA 92697-2715, USA. Email: cmccrimm@uci.edu (C.M.M.)/znenadic@uci.edu (Z.N.) and An H. Do, Department of Neurology, University of California Irvine, 101 The City Drive, Orange, CA 92868, USA. Email: and@uci.edu

Abstract

While prior noninvasive (e.g., electroencephalographic) studies suggest that the human primary motor cortex (M1) is active during gait processes, the limitations of noninvasive recordings make it impossible to determine whether M1 is involved in high-level motor control (e.g., obstacle avoidance, walking speed), low-level motor control (e.g., coordinated muscle activation), or only nonmotor processes (e.g., integrating/relaying sensory information). This study represents the first invasive electroneurophysiological characterization of the human leg M1 during walking. Two subjects with an electrocorticographic grid over the interhemispheric M1 area were recruited. Both exhibited generalized γ-band (40–200 Hz) synchronization across M1 during treadmill walking, as well as periodic γ-band changes within each stride (across multiple walking speeds). Additionally, these changes appeared to be of motor, rather than sensory, origin. However, M1 activity during walking shared few features with M1 activity during individual leg muscle movements, and was not highly correlated with lower limb trajectories on a single channel basis. These findings suggest that M1 primarily encodes high-level gait motor control (i.e., walking duration and speed) instead of the low-level patterns of leg muscle activation or movement trajectories. Therefore, M1 likely interacts with subcortical/spinal networks, which are responsible for low-level motor control, to produce normal human walking.

Key words: ECoG, electrophysiology, motor control, neurophysiology, walking

Introduction

Human gait is characterized by a repeating temporal pattern of coordinated muscle activity that changes in frequency with walking speed (Perry 2010). It has been hypothesized that the central and peripheral nervous systems interact in the following manner to produce these patterned movements: (1) mechanoreceptors

in the skin and muscles send afferent signals to the brain and spinal cord central pattern generators (CPGs) as well as modulate the activity of specific muscle groups through reflex arcs (Sinkjær et al. 2000; Dietz 2003; Rossignol et al. 2006), (2) the brain uses this peripheral sensory information along with visual and vestibular input to generate useful descending control signals (Rossignol et al. 2006), and (3) spinal CPGs then integrate this descending (brain) and ascending (sensory) input to ultimately produce the coordinated pattern of muscle contractions necessary for walking (Duysens and Van de Crommert 1998; Dietz 2003).

There is strong evidence supporting the role of spinal CPGs in human gait (Forssberg 1986; Bussel et al. 1988; Calancie et al. 1994; Dimitrijevic et al. 1998; Angeli et al. 2014). While supraspinal control also appears to be important for bipedal locomotion (Eidelberg 1981; Dietz 2003), the exact mechanism by which supraspinal centers control gait is not yet fully understood. Some human studies (Nathan 1994; Petersen et al. 2001) have suggested that intact function of the M1 is necessary for walking, while others (Masdeu et al. 1994; Hanna and Frank 1995) have suggested that only intact brainstem function is required. Nevertheless, it is likely that these supraspinal centers provide high-level commands to spinal CPGs during gait (Duysens and Van de Crommert 1998; Dietz 2003), instead of directly activating spinal motor neurons as proposed by Nielsen (2003) and Drew et al. (2008). This allows the brain to focus on other tasks, such as avoiding obstacles (Dietz 2003; Drew et al. 2004), while the CPGs carry out the low-level control of individual lower extremity muscles. However, a minimum level of input from the brain, specifically the frontal lobe, may still be required to maintain gait, since an individual's gait speed decreases when they perform a simultaneous cognitively demanding task (Yogev-Seligmann et al. 2008).

Neuroimaging studies have provided limited insight into the characteristics of supraspinal gait control in humans. For example, early studies reported on increased blood flow in the medial primary sensorimotor area during human gait (Fukuyama et al. 1997, la Fougère et al. 2010). These results were corroborated with near-infrared spectroscopy, where increases in total and oxygenated hemoglobin were observed over the primary sensorimotor area and the supplementary motor area (SMA) in response to execution and imagination of human gait (Miyai et al. 2001). Similarly, Christensen et al. (2000) demonstrated that leg bicycle movements were associated with increased perfusion of leg M1 and SMA areas. However, these neuroimaging approaches are generally incompatible with upright walking and lack the temporal resolution to study human gait at the time scale of individual steps.

Electrophysiological studies on the supraspinal control of human gait have also demonstrated involvement of the sensorimotor cortex (Wieser et al. 2010; Seeber et al. 2014, 2015). Leg M1 desynchronization in the μ (8–13 Hz) and β (14–40 Hz) bands has been observed during walking tasks (Wieser et al. 2010; Seeber et al. 2014), and even coherence between the β band and leg electromyogram (EMG) (Petersen et al. 2012). Gwin et al. (2011) and Seeber et al. (2015) described cyclic μ-, β-, and γ-band modulation throughout the gait cycle. Haefeli et al. (2011) observed modulation of cortical potentials (<30 Hz) during treadmill walking with an obstacle avoidance task. However, all of these studies utilized noninvasive electroencephalography (EEG), which has significant spatiotemporal resolution limitations and is highly susceptible to artifacts. The lack of spatial resolution makes it difficult to definitively identify what areas of the brain are involved in supraspinal gait control. In addition, EEG's limited temporal resolution (caused by the skull's high frequency attenuation; Niedermeyer and da Silva 2005) as well as its susceptibility to

biological artifacts such as eye blinks, ocular movements, and EMG contamination (Whitham et al. 2007; Ball et al. 2009; Schalk and Leuthardt 2011) undermine our ability to determine whether the γ-band modulation in some of the above studies is truly indicative of cortical activity rather than artifacts. Furthermore, mechanical artifacts caused by walking can result in wideband EEG power changes and may have influenced these studies' findings (Castermans et al. 2014; Kline et al. 2015). Collectively, these limitations make it difficult to draw any definitive conclusions from existing electrophysiological gait studies.

Many of these limitations can be overcome through the use of invasive electrophysiological recording techniques. For example, the subdural placement of electrodes in electrocorticography (ECoG) provides a more direct measure of cortical activity with high temporal and spatial resolution, while eliminating the possibility of correlated EMG contamination (Leuthardt et al. 2004). In addition, the effects of eye blinks, ocular movements, and motion artifacts are significantly reduced (Ball et al. 2009; Rao and Scherer 2010). However, invasive techniques have not yet been used to study human gait. Two prior studies (Miller et al. 2007; Ruescher et al. 2013) utilized ECoG to characterize cortical activity during isolated leg movements, and observed increased γ activity in the interhemispheric sensorimotor cortex. However, it remains unclear if and to what extent these findings generalize to gait tasks.

In summary, prior studies generally suggest that the human motor cortex plays a role in gait processes, but it is still unclear whether this role involves high-level control (obstacle avoidance, direction changes, walking speed, etc.), low-level control (over individual lower motor neurons), or processing and relaying sensory information to other regions (e.g., basal ganglia, thalamus, cerebellum). To answer some of these questions while avoiding the limitations of noninvasive techniques, we recorded ECoG from the cortical leg motor areas of human subjects as they performed various gait-related tasks. The resulting data were analyzed to determine: (1) the extent of cortical involvement in human gait, (2) what parameters of walking it encodes (e.g., gait duration, stepping rate, lower limb muscle activity/trajectories), and (3) to what extent this cortical activity represents motor control rather than sensory feedback or motion artifact.

Materials and Methods

The study was approved by the Institutional Review Boards of the University of California, Irvine and the Rancho Los Amigos National Rehabilitation Center. Subjects who were clinically implanted with an ECoG grid covering their leg M1 area for epilepsy surgery evaluation were recruited for the study. Those with a history of gait deficits or musculoskeletal disease were excluded from participation. It should be emphasized that the placement of the grids was solely determined by clinical indication and was in no way influenced by our study.

Data Collection

To minimize interference with clinical data acquisition, ECoG signals were split at the headbox and simultaneously routed to the clinical and research data acquisition systems. The research system utilized a NeXus-32 bioamplifier (Mind Media) to sample signals at a rate of 2048 Hz from up to 32 ECoG electrodes. ECoG signals were visually inspected, and those exhibiting excess noise were disconnected from the amplifier. Movement trajectories were simultaneously recorded from the hip, knee, ankle, and arm

on the side contralateral to the ECoG grid. Specifically, a custom-made electrogoniometer (Wang et al. 2011) was mounted over the dorsal aspect of the ankle to measure dorsiflexion/plantarflexion. In addition, 3 gyroscopes (L3GD20, STMicroelectronics) were mounted over the distal femoral, tibial, and humeral shafts in order to measure hip, knee, and shoulder flexion/extension, respectively. These trajectory data were acquired at 256 Hz by an integrated microcontroller (Arduino, Smart Projects). The ECoG and trajectory data were aligned using a common pulse train that was sent to both the bioamplifier and microcontroller systems. All signals were recorded while subjects performed the movement tasks described below. It should be noted that subjects participated in the experiments only after their seizures had been clinically localized and they had been placed back on anti-epileptic medication. This minimized the likelihood of seizures occurring during the experiment. Additional safety measures included the use of a bodyweight support system (Biodex Medical Systems) during the arm-swing and walking tasks (described below) in order to prevent falls.

Control Experiments

One of the goals of this study was to compare the spatial distribution of motor cortical activity during gait and during isolated limb movements, so the following control experiments were completed. Subjects performed 50 cycles of flexion and extension (with an intervening 3–5 s pause between movements) of the hip and knee contralateral to the ECoG grid while in a semirecumbent position. Subjects were instructed to remain motionless (idle) for ~30 s before the first and after the last movement cycle. A similar task was performed for ankle dorsiflexion and plantarflexion. Subjects also performed an isolated arm-swing task, in which they stood on the treadmill and alternated between remaining motionless (6 intervals, ~30 s each) and reciprocally swinging their arms (5 intervals, ~30 s each), as during walking but without leg movements.

Casual Walking Experiment

While standing on a treadmill with 0% weight-support applied, subjects alternated between remaining motionless (6 intervals, ~30 s each) and walking at a casual speed (5 intervals, ~30 s each). This casual speed was empirically chosen for each subject to maximize comfort and was used in all subsequent walking tasks.

Variable-Speed Walking Experiment

Subjects performed treadmill walking at the following speeds (30 s intervals each): casual, fast, casual, slow, casual, fast, casual, slow, casual. The slow and fast speeds were 50% and 150% of the casual speed, respectively. Subjects were instructed to stand motionless for ~30 s before the first and after the last walking interval.

Data Analysis

Electrode Localization

First, a 3D rendering of the T1 post-implantation magnetic resonance imaging (MRI) sequence was generated. ECoG electrode locations were determined from prominent electrode artifacts in the image (Hargreaves et al. 2011). Anatomical features were used to define M1 and surrounding brain regions (Wang et al. 2016). These regions were used to interpret the results of subsequent analyses.

Signal Processing

For every movement task, trajectory data were upsampled to 2048 Hz and temporally aligned with the ECoG data. The raw ECoG signal from each electrode was common-average referenced and then processed in the following manner. First, to remove any DC component as well as line noise (60 Hz) and its harmonics, a high-pass filter (0.05 Hz cutoff) and stopband filters (57–63, 117–123, and 177–183 Hz) were applied. The resulting signal was then filtered into the following physiological bands: μ (8–13 Hz), β (14–40 Hz), and γ (40–200 Hz). These signals were squared and low-passed (3 Hz cutoff) to generate band-specific power envelopes, P_μ, P_β, and P_γ. An example is provided in Figure 1, along with a picture of the setup. Short (<10 ms) electrode disconnect artifacts that were occasionally observed in the raw ECoG data were replaced by interpolation in the power envelope data. Segments that contained longer capacitive discharge artifacts were discarded.

Control Experiment Data

To analyze the motor cortical changes that occurred during the isolated hip, knee, ankle, and arm-swing movement tasks, the following steps were performed. Angular velocity time series (ω) were derived from the appropriate kinematic sensor during these tasks and used to identify instances of flexion/dorsiflexion (ω ≫ 0°/s) and extension/plantarflexion (ω ≪ 0°/s). Then P_μ, P_β, and P_γ for each electrode were segmented into these events. Since each subject participated in 50 flexion and 50 extension events, there were 50 power envelope segments for flexion and 50 power envelope segments for extension in each of the μ, β, and γ bands. Next, for each physiological band, we calculated the increase in power during each flexion and extension segment (relative to idling), which we refer to as the synchronization index (details in Supplementary Material 1.1). Note that the synchronization index is positive for cortical synchronization and negative for cortical desynchronization. Electrodes where the central 95% of synchronization indices across all flexion or across extension segments were >0 (synchronization) or <0 (desynchronization) were defined as having exhibited consistent changes.

Walking Experiment Data

To determine if the subjects exhibited motor cortical changes during walking (relative to idling), the following analysis was performed for the casual walking task. First, data from the tibial gyroscope were used to delineate individual gait cycles, or strides, by identifying the point of initial contact (Aminian et al. 2002). The corresponding walking task P_μ, P_β, and P_γ were segmented into these strides for each electrode. Then, the increase in power during each stride relative to standing motionless (i.e., the synchronization index) was calculated for every electrode and physiological band (details in Supplementary Material 1.1). Likewise, electrodes where the central 95% of synchronization indices across all strides were completely above or below 0 were defined as having exhibited consistent walking-related changes.

While the above analysis may elucidate generalized increases/decreases in cortical activity during walking, we also examined whether the cortical activity exhibited periodic changes within every stride. To this end, we calculated the ratio of the dominant frequency of P_μ, P_β, and P_γ to the stepping rate for each 30-s movement interval from the variable-speed walking task (details in Supplementary Material 1.2). These ratios are referred to as R_μ, R_β, and R_γ. Note that the dominant frequencies and stepping rates were determined for each interval as the frequencies where the
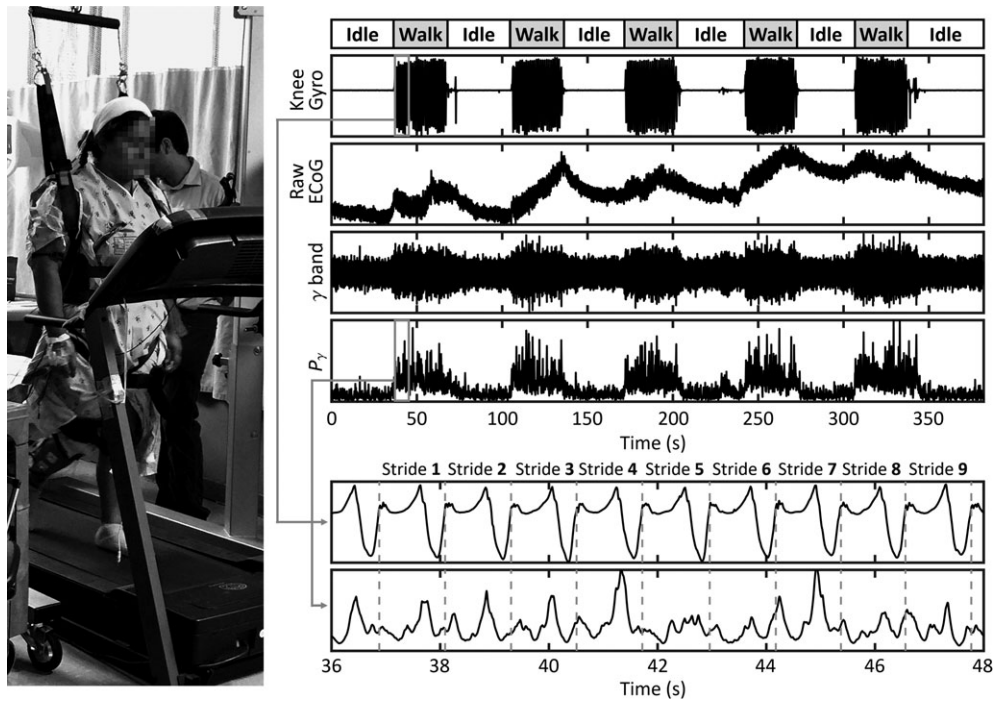
Figure 1. Example of the experimental setup and signal processing steps for the casual walking task. This task was comprised of 6 intervals of idling (each ~30 s long), in which the subject stood motionless, interspersed with 5 intervals of walking (each ~30 s long). Data from the tibial shaft's gyroscope (contralateral to the ECoG grid) provided the trajectory of knee flexion/extension. ECoG data from one electrode is shown in its raw, γ-band filtered, and γ-band power envelope forms. A close-up of the knee gyro and P_γ signals around the 40 s mark demonstrates the segmentation of these signals into individual gait cycles (strides).

power spectral density (PSD) of P_μ, P_β, P_γ, and hip angular velocity (ω) were maximal. An integer R value is indicative of cortical intrastride modulation that repeats every gait cycle. For example, an electrode that consistently exhibits an R value of ~1 indicates that there is a single, time-locked burst in nearby cortical activity per gait cycle, regardless of the walking speed.

To determine whether the cortical activity observed during walking represents supraspinal control of individual lower extremity muscle groups or trajectories, the following analyses were performed. First, every gait cycle from the casual walking task was broken into 7 phases (Perry 2010). These phases comprised loading response (0–12% of the gait cycle duration), mid stance (12–31%), terminal stance (31–50%), pre-swing (50–62%), initial swing (62–75%), mid swing (75–87%), and terminal swing (87–100%). Then, we compared the spatial pattern of cortical activity during each gait cycle phase to the cortical activity patterns from the isolated movements associated with each phase (e.g., ankle plantarflexion for mid stance, hip flexion, and ankle dorsiflexion for mid swing). Next, since prior studies have observed high correlations between single ECoG electrodes and upper-limb trajectories (Wang et al. 2013a), we evaluated whether single electrodes from the leg M1 area encode lower extremity trajectories during gait. To this end, we calculated the lag-optimized Pearson correlation coefficients between P_μ, P_β, P_γ and hip, knee, ankle ω over all walking intervals using a phase offset in the [–0.5 s, 0.5 s] range.

Finally, to determine if any of the observed cortical changes were caused by sensory feedback or movement artifacts, the following steps were performed. First, we analyzed the temporal relationship between onset of gait movements and the onset of cortical synchronization or desynchronization during the casual walking task. Due to the periodic nature of walking, it is difficult to temporally disentangle motor and sensory

components of ECoG, so we focused our analysis on the transitions from idling to walking. We chose electrodes that displayed large changes in the μ, β, or γ band and analyzed the average P_μ, P_β, or P_γ waveform, respectively, around the onset of walking. In each physiological band, any walking-related cortical changes that precede the onset of movement are more indicative of motor intention than sensory/proprioceptive feedback. Next, we compared the PSD of hip ω with the PSD of the raw ECoG data from each electrode (see Supplementary Fig. 2). Briefly, any frequencies where the peaks in the raw ECoG PSD matched the harmonic peaks of hip movement were likely contaminated by movement artifacts.

Results

Subjects

Two subjects, SJ1 (F, 32 y.o.) and SJ2 (F, 38 y.o.), gave their informed consent to participate in the study. Both had been implanted with an 8 × 4 high-density array of platinum-iridium ECoG electrodes (Integra LifeSciences) with a 2 mm diameter and a 4 mm center-to-center interelectrode spacing (Fig. 2). Note that these high-density electrode grids have superior spatial resolution and signal quality compared with standard ECoG grids (Kellis et al. 2016; Wang et al. 2016). The electrode locations, determined by MRI, are displayed in Figure 2. SJ1's grid and SJ2's grid were located on the left and right hemisphere, respectively. Each subject had ≥16 electrodes positioned over the leg M1 area. Due to excess noise contamination, a total of 3 electrodes (21, 25, 26) from SJ1 and 4 electrodes (18, 20, 21, 24) from SJ2 remained disconnected from the research system for the duration of the experiment. The casual and variable-speed walking data from these disconnected electrodes were recovered from the clinical
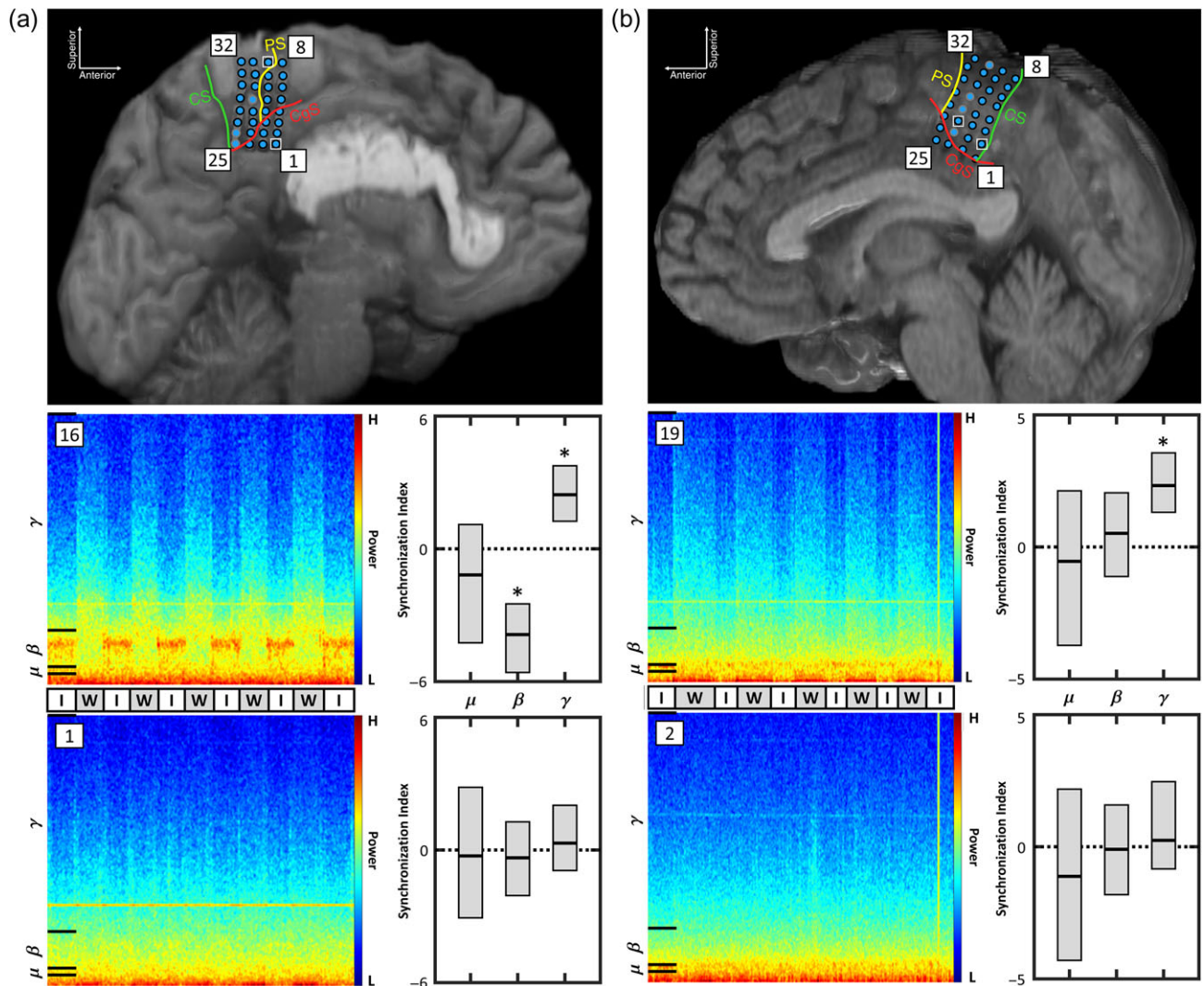
Figure 2. The location of the interhemispheric ECoG grid electrodes in SJ1 (a) and SJ2 (b) are depicted. Research data were collected from electrodes outline in black. Electrodes outlined in gray were disconnected from the research system for the duration of the study, and their walking data were recovered from the clinical system. The central sulcus (CS), precentral sulcus (PS), and cingulate sulcus (CgS) are delineated. Also note the presence of a large pericallosal lipoma in SJ1. Some electrodes in each subject, such as SJ1's M1 electrode 16 and SJ2's M1 electrode 19, exhibited an increase in γ power during walking (W) compared to idling (I). Other electrodes in each subject, such as SJ1's electrode 1 and SJ2's electrode 2, exhibited no walking related changes. Spectrograms from the casual walking tasks are shown for these electrodes along with the empirical 95% intervals for the synchronization indices across strides in the μ, β, and γ bands. Note that bands where these intervals did not cross zero were defined to have exhibited consistent synchronization or desynchronization (*).

system and aligned to the research data for analysis. However, the sampling rate of the clinical system was 512 Hz for SJ1 and only 256 Hz for SJ2, so, for SJ2's electrodes 18, 20, 21, and 24, the γ band was defined as 40–127 Hz (with 128 Hz being the Nyquist limit). To ensure that this approximation was valid, the P_γ was calculated as in "Signal Processing" section for the remaining electrodes, that is, those connected to both the research system and the clinical system. For electrodes that exhibited substantial walking-related power modulation, a high degree of similarity (median correlations of 0.98 for SJ1 and 0.91 for SJ2) between the research and clinical P_γ data was observed (see Supplementary Material 2.1).

SJ1 participated in the control experiments (hip, knee, ankle, and arm-swing), as well as the casual walking task (twice) and variable-speed walking task (twice). Due to fatigue and lack of availability, SJ2 only completed the isolated hip, knee, and ankle movements (no arm-swing), and participated in the

casual walking task and variable-speed walking task only once each. The casual walking speeds for SJ1 and SJ2 were empirically chosen as 2 and 1 mph, respectively. This discrepancy was due to SJ2's smaller stature and her not being comfortable walking at higher speeds. Nevertheless, at these speeds, toe-off for SJ1 and SJ2 typically occurred around 61% and 60% of the gait cycle, respectively. These closely match the expected value (62%) for casual walking (Perry 2010). No epileptic discharges were found upon inspection of both subjects' experimental data. A total of 9 artifacts (3 short and 6 long) were identified in SJ1's and SJ2's data, mostly during idling intervals, and were removed as described in Signal Processing section.

Control Experiment Data

Both subjects exhibited consistent μ and γ changes in several electrodes during flexion and extension of the hip, knee, and

ankle. These changes were typically observed over the inter-hemispheric M1 and SMA. Neither subject exhibited extensive β changes during the isolated leg movements; consistent changes were only observed during hip flexion (SJ1: electrode 6), knee flexion (SJ1: electrodes 7, 16, 24; SJ2: electrode 22), and knee extension (SJ2: electrode 22). As expected from classic neurophysiology, no consistent μ, β, or γ changes were observed in any of SJ1's electrodes during the arm-swing task.

Walking Experiment Data

Spectrograms are provided in Figure 2, along with the empirical 95% intervals for the μ-, β-, and γ-band synchronization indices, for 2 electrodes from each subject during the casual walking task. During this task, SJ1 exhibited consistent walking-related changes across strides in the μ (electrodes 22, 30), β (electrodes 3–4, 6, 8–12, 14–19, 21–24, 26–27, 31–32), and γ (electrodes 3–32) bands. SJ2 exhibited consistent walking-related changes in only the γ band (electrodes 3–4, 7–8, 10–16, 19–21, 23–24, 27–29, 31–32). These cortical changes were concentrated over M1 in both subjects (see Supplementary Fig. 1).

In addition to exhibiting a generalized increase/decrease in activity during walking (relative to idling), 7 of SJ1's electrodes also showed intrastride modulation ($R \approx 1$ or $R \approx 2$) from at least 89% (16/18) of the variable-speed walking intervals (Fig. 3). Six of these electrodes were located over M1, while one was located over the SMA. All of the electrodes exhibited only γ-band intrastride modulation, except for electrode 32 which exhibited both β and γ-band intrastride modulation. For SJ2, 7 electrodes also exhibited intrastride modulation from at least 89% (8/9) of the variable-speed walking intervals. All of these electrodes were located over M1, and all exhibited only γ-band intrastride modulation. Of the electrodes that showed periodic changes within the gait cycle, electrodes 14, 16, and 24 from SJ1 and electrodes 7, 15, and 21–24 from SJ2 typically exhibited $R_\gamma \approx 1$ across walking intervals, while electrode 19 from SJ2 exhibited $R_\gamma \approx 2$. Four electrodes from SJ1, electrodes 22–23 and 31–32, displayed no obvious preference for either $R_\gamma \approx 1$ or $R_\gamma \approx 2$ (see electrode 32 from SJ1 in Fig. 3). However, these electrodes generally exhibited $R_\gamma \approx 1$ during slower walking and $R_\gamma \approx 2$ during faster walking. The 1 or 2 bursts in cortical γ-band activity per gait cycle, represented by $R_\gamma \approx 1$ or $R_\gamma \approx 2$, typically occurred around the swing-to-stance transition (0%) and/or stance-to-swing transition (50–62%) for both subjects (see Supplementary Fig. 3). Note that there did not appear to be consistent relationship between amplitude of these P_γ bursts and walking speed (i.e., a few of SJ1's electrodes showed an increase in P_γ burst amplitude with faster walking, but we did not observe this effect in SJ2).

Although the terminal stance phase of gait primarily involves the ankle plantarflexors (especially the gastrocnemius and soleus muscles), the spatial distribution of cortical γ-band activity during terminal stance showed no obvious similarity to the spatial distribution of cortical γ activity during isolated ankle plantarflexion (Fig. 4a). This was also true for the preswing and hip flexion (Fig. 4b), as well as for mid swing and hip flexion and ankle dorsiflexion (Fig. 4c). The correlation analysis between P_μ, P_β, P_γ and hip, knee, ankle ω over all walking intervals produced no correlation coefficients above $r = 0.5$. The highest correlations observed were between P_β and knee ω ($r = 0.48$) for SJ1 and between P_γ and hip ω ($r = 0.42$) for SJ2. The lags associated with these maximum correlations were −180 and −305 ms suggesting that these P_β and P_γ signals preceded knee and hip ω.

Synchronization in the γ band in both subjects clearly preceded the onset of movement (see Fig. 5). In addition, the PSD of the raw ECoG data from both subjects displayed peaks up to ~10 Hz that corresponded to super-harmonics of the stepping rate (see Supplementary Fig. 2). Thus, although the μ band may have been partially contaminated by movement artifacts, it is unlikely that the β and γ bands were affected.

Discussion

This study provides the first invasive electroneurophysiological characterization of M1 activity during human walking. The results above suggest that this region is involved in high-level gait processes. Specifically, M1 exhibits recognizable electrophysiological changes between standing and walking as well as within each stride (regardless of walking speed), thereby encoding both gait duration and gait speed. Moreover, this activity likely represents motor intention instead of sensory/proprioceptive information, but does not robustly encode lower extremity muscle/trajectory control during gait at the level of single electrodes. This further supports the idea that M1 interacts with downstream networks, such as CPGs, to produce the coordinated leg movements that comprise normal gait.

Figure 3. Electrodes in SJ1 and SJ2 that demonstrated intrastride μ, β, or γ modulation during ≥89% of the variable-speed walking intervals are colored white; otherwise, they are colored dark gray. The R_μ, R_β, and R_γ values (dots) from each 30-s walking interval are displayed for SJ1's electrodes 32 and 19 and for SJ2's electrodes 23 and 19. Recall that R_μ is the ratio of the dominant bursting frequency in the μ band to the stepping frequency, and similarly for R_β and R_γ with the β and γ bands, respectively. The plotted R values are ordered in the y-axis according to their corresponding stepping rate, with the R value from the 30-s interval with fastest stepping rate on top. The horizontal gray lines separate the R values from fast (top), casual (middle), and slow (bottom) walking intervals. The percentage of intervals with R_μ, R_β, or R_γ values near 1 or 2 (± 0.05) is provided.

Control Experiments

As expected from previous studies (e.g., Miller et al. 2007 and Ruescher et al. 2013), the modulation of neural activity over interhemispheric M1 during hip, knee, and ankle movements suggests that isolated lower extremity movements are under cortical control. As with these prior studies, we also observed that the spatial distribution of the hip, knee, and ankle motor
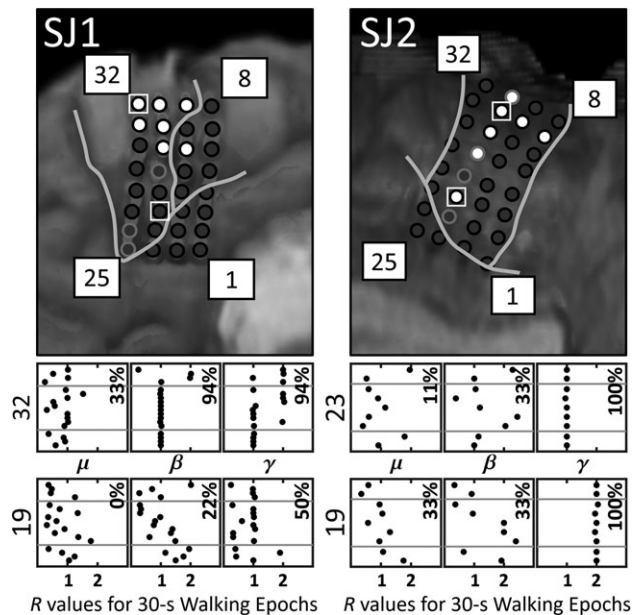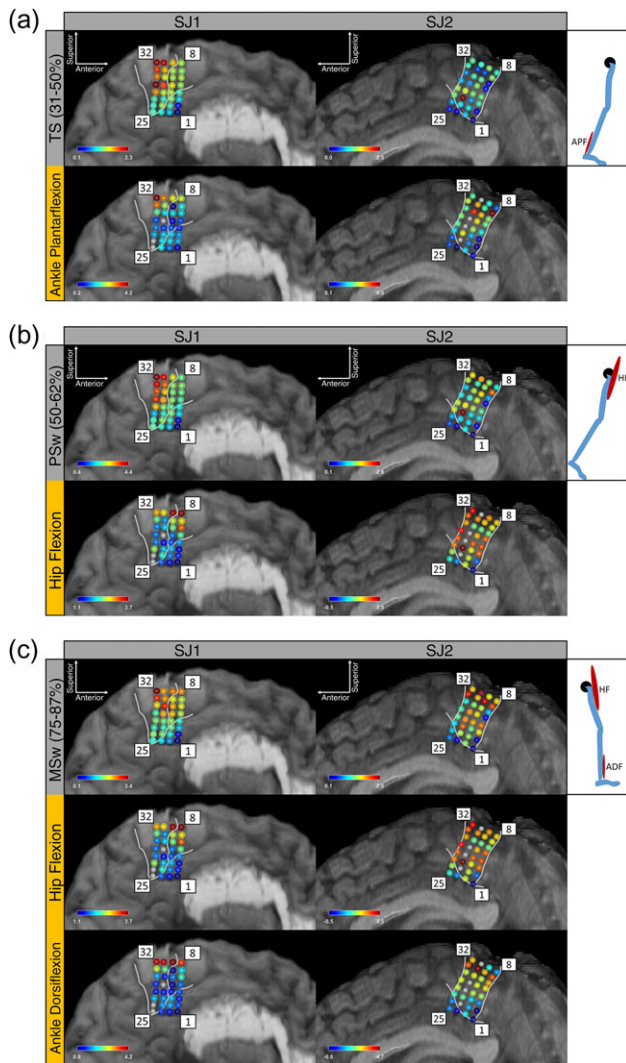
Figure 4. Subject SJ1's and SJ2's increase in γ-band power (average synchronization index) during: (*a*) terminal stance (TS) and isolated ankle plantarflexion (APF), (*b*) preswing (PSw) and isolated hip flexion (HF), and (*c*) mid swing (MSw) as well as isolated hip flexion and ankle dorsiflexion (ADF). Each of the phases pictured (terminal stance, pre-swing, and mid swing) is displayed above the control experiment data from the muscle group(s) that are active during that phase of the gait cycle. Data from a SJ1's electrodes 21, 25, 26 and SJ2's electrodes 18, 20, 21, 24 were recovered for the casual walking task but not for the control experiments. Note the differences in the spatial distribution of motor cortical activity for gait and non-gait movements that utilized the same muscle group(s). Quantitatively, the adjusted-r^2 values for each phase's cortical activity as a linear combination of the relevant control experiments' cortical activity were 0.30, 0.07, 0.34 (SJ1) and 0.01, 0.35, 0.46 (SJ2) for terminal stance, preswing, and mid swing, respectively.

representation areas did not necessarily conform to the classical somatotopy of the motor homunculus (with superior-to-posterior orientation; Penfield and Rasmussen 1950). However, unlike in Miller et al. (2007), we observed: (1) an increase in interhemispheric γ-band activity during ankle movements, and (2) no consistent interhemispheric changes in the μ, β, or γ band during arm movements (arm-swing).

Walking Experiments

This is the first study that measured cortical activity from subdural electrodes during human gait, and our results provide
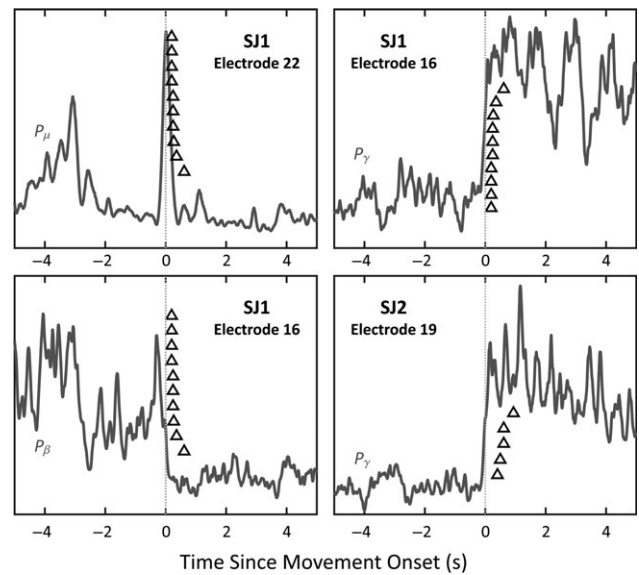

Figure 5. The temporal relationship between changes in the μ, β, and γ band and the onset of movement (black triangles). A few examples of the average $P_μ$, $P_β$, or $P_γ$ waveforms from when the subjects transitioned from standing motionless to walking during the casual walking experiment are provided. Time zero (vertical gray line) is when the treadmill first started moving. The black triangles indicate the time that the subjects began walking (first lower extremity gait movement) for each 30-s interval (10 for SJ1 and 5 for SJ2). Note that SJ1's and SJ2's $P_γ$ synchronization typically preceded the onset of movement by a few hundred milliseconds (average of 273 ms for SJ1 and 603 ms for SJ2).

direct evidence that M1 encodes walking parameters. This is aligned with prior animal studies, which suggest that supraspinal signals (Forssberg and Grillner 1973; Pearson and Rossignol 1991; Barbeau et al. 1993), possibly of motor cortical origin (Armstrong and Drew 1984a,b; Leblond et al. 2001; Prilutsky et al. 2005), contribute to locomotor control, especially for volitional, high-level gait modifications (Beloozerova and Sirota 1993; Drew et al. 1996). Note that although no direct comparison has been made, many studies (Eidelberg 1981; Vilensky 1987; Armstrong 1988; Vilensky and O'Connor 1998; Capaday 2002; Dietz 2003; Nielsen 2003) have hypothesized that primates (especially humans) rely on these corticospinal pathways for locomotor control to an even greater extent than low animals. Our observation that much of the interhemispheric M1 undergoes generalized γ-band synchronization upon initiating walking was consistent across subjects, and is somewhat analogous to the γ-band synchronization seen in prior human studies during individual upper and lower extremity movements (Crone et al. 1998; Pfurtscheller et al. 2003; Miller et al. 2007; Ruescher et al. 2013; Wang et al. 2013a). The observed γ-band synchronization was maintained throughout the entirety of each 30-s walking interval, and did not occur solely at the onset of movement. Thus, it is unlikely that cortical involvement is only required at the onset of walking to facilitate initial activation of the CPGs. However, it remains unclear whether this M1 activity is related to mesencephalic locomotor region activity, which may be involved in quadruped locomotor initiation (Mori 1987; Whelan 1996). In addition, while SJ1 exhibited μ- and β-band desynchronization in M1 during walking, SJ2 did not, so these features of gait may be less consistent across individuals. Alternatively, SJ2 may have been strongly utilizing her leg muscles to maintain her balance during idling such that further desynchronization during walking was reduced. In contrast, Seeber et al. (2014, 2015) allowed subjects to completely relax

their muscles during standing by mounting them in a robotic gait orthosis with body weight support, and observed consistent μ and β EEG desynchronization.

In addition to undergoing generalized synchronization during walking, M1 γ-band activity was time-locked to the gait cycle across a range of walking speeds, thereby indicating that this cortical area encodes gait speed. This agrees with previous findings in animals (e.g., Armstrong and Drew 1984a), and suggests that the cortex may provide input to downstream networks at specific times in the gait cycle. One possible explanation for the observation that electrodes in SJ1 exhibited one burst in γ-band activity per stride during slower walking and 2 bursts per stride during faster walking (see Fig. 3) is that individual M1 neurons switch their bursting regime at higher speeds. Specifically, since human spinal networks are able to produce a variety of locomotor patterns (Danner et al. 2015), it is possible that different supraspinal inputs to the CPGs during slow and fast walking (different number of bursts per gait cycle) are required to alter one's gait biomechanics. Note that although SJ2 did not exhibit this transition from $R_\gamma \approx 1$ to $R_\gamma \approx 2$ with faster walking, her overall walking speed was substantially slower than SJ1's (1 mph vs. 2 mph for casual walking). Although oscillations in the β and μ bands may be associated with changes in muscle activation (Hansen and Nielsen 2004; Raethjen et al. 2008; Petersen et al. 2012; van Wijk et al. 2012), only one electrode in one subject (SJ1) showed consistent intrastride β modulation, and no electrode in either subject showed consistent intrastride μ modulation. Therefore, our study did not find evidence to support that the M1 μ band encodes walking speed. In addition, the β-band intrastride modulation observed in a single electrode in SJ1 may actually reflect changes in the lower end of the γ band (~40 Hz). Note that Figure 2a shows desynchronization up to ~35 Hz, so the 35–40 Hz range may be dominated by physiological γ signals.

Studies by Schubert et al. (1997) and Capaday et al. (1999) suggest that the ankle dorsiflexors are more susceptible to facilitation via transcranial magnetic stimulation than the ankle plantarflexors, possibly due to the flexor dominance of the motor cortex reported in the literature (Brouwer and Ashby 1992; Dietz 2003). However, as seen in Figure 4, neither ankle plantarflexion, hip flexion, or ankle dorsiflexion elicited the same spatiotemporal patterns during walking as when performed individually, suggesting that cortical control of lower extremities is different in each condition. Additionally, unlike upper extremity trajectories which exhibit correlation coefficients of $r > 0.8$ at the level of single channels (Wang et al. 2013a), we only observed modest correlations ($r < 0.5$) between cortical P_μ, P_β, P_γ and hip, knee, ankle ω. This indicates that lower limb trajectories during gait are not as robustly encoded at the level of single ECoG electrodes. One plausible interpretation of these findings is that M1 provides rhythmic input to spinal CPGs, rather than directly activating motor neurons, during walking. Moreover, our results in Supplementary Fig. 3 suggest that this cortical activity is time-locked to initial contact and/or preswing. This type of bimodal, supraspinal signal could act as a pacing signal for CPGs to: (1) carry out ipsilateral and contralateral heel strike, (2) activate certain muscles (e.g., ankle dorsiflexors), or (3) release inhibition of other motor or obstacle avoidance pathways, which may explain why cortical stimulation only at specific times of the gait cycle facilitates lower extremity muscle activity (Schubert et al. 1997; Capaday et al. 1999).

Our results in Figure 5 indicate that the observed M1 γ-band activity was not caused by sensory feedback, and is therefore likely related to motor intention. In addition, our findings do not appear to be influenced by movement artifacts. Suspected motion artifacts were present in the raw ECoG and gyroscope data up to ~10 Hz, possibly from cable or electrode movements. This observation is consistent with prior EEG studies (Castermans et al. 2014). Since the β and γ bands were unaffected, the above results for these bands were not likely caused by movement artifacts. Furthermore, it is unlikely that the μ desynchronization was caused solely by movement artifacts, since a decrease, rather than an increase, in power was observed during walking.

Comparison to Previous Studies

All previous studies on the brain electrophysiology of human gait have utilized noninvasive recording modalities, with most studies using EEG. Since EEG is prone to contamination by motion artifacts, many studies sought to remove these artifacts through various methods, such as independent (Gwin et al. 2011) or spectral (Seeber et al. 2015) component analysis. However, it is difficult to determine how the resulting, highly processed signals in these studies relate to true physiological activity. Moreover, motion artifacts may still have been present in the data even after performing artifact rejection (Kline et al. 2015).

Many of the previous EEG gait studies observed wideband (μ, β, γ) modulation (Gwin et al. 2011; Seeber et al. 2014, 2015) that appeared to be temporally locked to the gait cycle. Specifically, these studies observed components of EEG from the leg sensorimotor area with 2 wideband bursts per gait cycle that typically occurred at times of double-leg support (0–12% and 50–60% of the gait cycle). On the other hand, Haefeli et al. (2011) performed a time-domain analysis by averaging EEG across multiple gait cycles during normal walking. They observed little cortical activity over the leg motor area, except possibly around the swing-to-stance transition. However, the EEG features in the above studies are also suggestive of motion artifact contamination (Castermans et al. 2014; Kline et al. 2015). In addition, it is unclear what the γ-band changes in these studies corresponded to, since EEG is temporally filtered by the skull (Niedermeyer and da Silva 2005) and has limited spatial resolution (e.g., signals can be smeared across hemispheres and across the primary sensory and motor areas). Without examining the raw data, it is impossible to determine whether these findings represent true brain physiology rather than biological or motion artifacts. In contrast, ECoG grids are much less sensitive to biological artifacts, such as ocular movements and EMG, due to their subdural placement. In addition, ECoG is expected to be less sensitive to motion artifacts than EEG (Ball et al. 2009), and this is supported by our observations. For example, movement artifacts that appeared as harmonics of the stepping rate were present in the ECoG data only up to ~10 Hz, even for fast walking. By comparison, these artifacts can be present in EEG data up to ~30 Hz (Castermans et al. 2014). Moreover, our data did not exhibit the wide band modulation that is characteristic of motion artifact contamination, and changes in both the β and γ bands preceded the onset of movement.

Currently, no studies have demonstrated that human walking speed is encoded by M1. In the closest study, Lisi and Morimoto (2015) used μ- and β-band features from EEG to determine when an individual's walking speed was changing. However, the authors did not show that the brain itself encodes gait speed nor identified any physiological features that were associated with changes in gait speed.

Limitations

The major limitation of this study was its small sample size ($n = 2$). However, it should be noted that interhemispheric ECoG

grid implantation for epilepsy surgery evaluation is extremely rare. For example, surgical epilepsy centers average only 2–3 interhemispheric grid implantations per year (Bekelis et al. 2012). Nevertheless, since we observed consistent features in both subjects (a stereotypical pattern of γ activity throughout each gait cycle that encodes walking as well as the stepping rate), it is reasonable to expect that these results could generalize to a larger population. Although the ECoG data in this study came from individuals with epilepsy, we expect that healthy subjects exhibit similar electrophysiological features in their motor cortices. First, the epileptic foci of both subjects were ultimately found to be localized to the temporal lobe, so it is unlikely that there were significant neuroplastic changes to M1. Secondly, the cortical features associated with movement in individuals with epilepsy, from this study as well as others (Crone et al. 1998; Pfurtscheller et al. 2003; Miller et al. 2007; Ruescher et al. 2013; Wang et al. 2013), are consistent with the electrophysiological features that underlie movement in individuals without epilepsy (Hochberg et al. 2012; Yanagisawa et al. 2012; Wang et al. 2013b; Aflalo et al. 2015). Another limitation was that the ECoG grids were confined to a small area of a single brain hemisphere. Hence, it was not possible to assess the involvement of other cortical areas. For example, both subjects had minimal coverage of the cingulate gyrus, and only SJ1 had electrodes over the SMA. Therefore, although the SMA also appeared to participate in encoding gait, additional subjects are needed to verify this. Similarly, elucidating the involvement of other cortical areas will require subjects with additional ECoG grid coverage. Finally, this study utilized treadmill walking, which may require increased cognitive effort from subjects compared with overground walking. This could be responsible for the substantial gait-related changes observed in M1. However, safety and space constraints precluded subjects from performing overground walking, and treadmill walking may still be a better model of normal gait than techniques from other studies (e.g., bicycle movements; Christensen et al. 2000 and weight-supported robotic orthosis walking; Seeber et al. 2014, 2015).

Supplementary Material

Supplementary data is available at *Cerebral Cortex* online.

Funding

Notes

Conflict of Interest: None declared.

References

Aflalo T, Kellis S, Klaes C, Lee B, Shi Y, Pejsa K, Shanfield K, Hayes-Jackson S, Aisen M, Heck C, et al. 2015. Decoding motor imagery from the posterior parietal cortex of a tetraplegic human. Science. 348:906–910.

Aminian K, Najafi B, Büla C, Leyvraz PF, Robert P. 2002. Spatiotemporal parameters of gait measured by an ambulatory system using miniature gyroscopes. J Biomech. 35:689–699.

Angeli CA, Edgerton VR, Gerasimenko YP, Harkema SJ. 2014. Altering spinal cord excitability enables voluntary movements after chronic complete paralysis in humans. Brain. 137:1394–1409.

Armstrong DM, Drew T. 1984a. Discharges of pyramidal tract and other motor cortical neurones during locomotion in the cat. J Physiol. 346:471–495.

Armstrong DM, Drew T. 1984b. Locomotor-related neuronal discharges in cat motor cortex compared with peripheral receptive fields and evoked movements. J Physiol. 346: 497–517.

Armstrong DM. 1988. The supraspinal control of mammalian locomotion. J Physiol. 405:1–37.

Ball T, Kern M, Mutschler I, Aertsen A, Schulze-Bonhage A. 2009. Signal quality of simultaneously recorded invasive and non-invasive EEG. Neuroimage. 46:708–716.

Barbeau H, Chau C, Rossignol S. 1993. Noradrenergic agonists and locomotor training affect locomotor recovery after cord transection in adult cats. Brain Res Bull. 30:387–393.

Bekelis K, Radwan TA, Desai A, Moses ZB, Thadani VM, Jobst BC, Bujarski KA, Darcey TM, Roberts DW. 2012. Subdural interhemispheric grid electrodes for intracranial epilepsy monitoring: feasibility, safety, and utility: clinical article. J Neurosurg. 117:1182–1188.

Beloozerova IN, Sirota MG. 1993. The role of the motor cortex in the control of vigour of locomotor movements in the cat. J Physiol. 461:27–46.

Brouwer B, Ashby P. 1992. Corticospinal projections to lower limb motoneurons in man. Exp Brain Res. 89:649–654.

Bussel B, Roby-Brami A, Azouvi P, Biraben A, Yakovleff A, Held JP. 1988. Myoclonus in a patient with spinal cord transection. Possible involvement of the spinal stepping generator. Brain. 11:1235–1245.

Calancie B, Needham-Shropshire B, Jacobs P, Willer K, Zych G, Green BA. 1994. Involuntary stepping after chronic spinal cord injury. Evidence for a central rhythm generator for locomotion in man. Brain. 117:1143–1159.

Capaday C, Lavoi BA, Barbeau H, Schneider C, Bonnard M. 1999. Studies on corticospinal control of human walking. I. Responses to focal transcranial magnetic stimulation of the motor cortex. J Neurophysiol. 81:129–139.

Capaday C. 2002. The special nature of human walking and its neural control. Trends Neurosci. 25:370–376.

Castermans T, Duvinage M, Cheron G, Dutoit T. 2014. About the cortical origin of the low-delta and high-gamma rhythms observed in EEG signals during treadmill walking. Neurosci Lett. 561:166–170.

Christensen LO, Johannsen P, Sinkjaer T, Petersen N, Pyndt HS, Nielsen JB. 2000. Cerebral activation during bicycle movements in man. Exp Brain Res. 135:66–72.

Crone NE, Miglioretti DL, Gordon B, Lesser RP. 1998. Functional mapping of human sensorimotor cortex with electrocorticographic spectral analysis. II. Event-related synchronization in the gamma band. Brain. 121:2301–2315.

Danner SM, Hofstoetter US, Freundl B, Binder H, Mayr W, Rattay F, Minassian K. 2015. Human spinal locomotor control is based on flexibly organized burst generators. Brain. 138:577–588.

Dietz V. 2003. Spinal cord pattern generators for locomotion. Clin Neurophysiol. 114:1379–1389.

Dimitrijevic MR, Gerasimenko Y, Pinter MM. 1998. Evidence for a spinal central pattern generator in humans. Ann N Y Acad Sci. 860:360–376.

Drew T, Jiang W, Kably B, Lavoie S. 1996. Role of the motor cortex in the control of visually triggered gait modifications. Can J Physiol Pharmacol. 74:426–442.

Drew T, Prentice S, Schepens B. 2004. Cortical and brainstem control of locomotion. Prog Brain Res. 143:251–261.

Drew T, Kalaska J, Krouchev N. 2008. Muscle synergies during locomotion in the cat: a model for motor cortex control. J Physiol. 586:1239–1245.

Duysens J, Van de Crommert HW. 1998. Neural control of locomotion; The central pattern generator from cats to humans. Gait Posture. 7:131–141.

Eidelberg E. 1981. Consequences of spinal cord lesions upon motor function, with reference of locomotor activity. Prog Neurobiol. 17:185–202.

Forssberg H, Grillner S. 1973. The locomotion of the acute spinal cat injected with clonidine iv. Brain Res. 50(1):184–186.

Forssberg H. 1986. A developmental model of human locomotion. In: Grillner S, Stein PSG, Stuart DG, Forssberg H, Herman RM, editors. . Wenner Gren international symposium series. Vol 45. London (UK): Macmillan. p. 485–501.

Gwin JT, Gramann K, Makeig S, Ferris DP. 2011. Electrocortical activity is coupled to gait cycle phase during treadmill walking. Neuroimage. 54:1289–1296.

Fukuyama H, Ouchi Y, Matsuzaki S, Nagahama Y, Yamauchi H, Ogawa M, Kimura J, Shibasaki H. 1997. Brain functional activity during gait in normal subjects: a SPECT study. Neurosci Lett. 228:183–186.

Haefeli J, Vogeli S, Michel J, Dietz V. 2011. Preparation and performance of obstacle steps: interaction between brain and spinal neuronal activity. Eur J Neurosci. 33:338–348.

Hanna JP, Frank JI. 1995. Automatic stepping in the pontomedullary stage of central herniation. Neurology. 45:985–986.

Hansen NL, Nielsen JB. 2004. The effect of transcranial magnetic stimulation and peripheral nerve stimulation on corticomuscular coherence in humans. J Physiol. 561:295–306.

Hargreaves BA, Worters PW, Pauly KB, Pauly JM, Koch KM, Gold GE. 2011. Metal-induced artifacts in MRI. Am J Roentgenol. 197:547–555.

Hochberg LR, Bacher D, Jarosiewicz B, Masse NY, Simeral JD, Vogel J, Haddadin S, Liu J, Cash SS, van der Smagt P, et al. 2012. Reach and grasp by people with tetraplegia using a neurally controlled robotic arm. Nature. 485:372–375.

Kellis S, Sorensen L, Darvas F, Sayres C, O'Neill K3rd, Brown RB, House P, Ojemann J, Greger B. 2016. Multi-scale analysis of neural activity in humans: implications for micro-scale electrocorticography. Clin Neurophysiol. 127:591–601.

Kline JE, Huang HJ, Snyder KL, Ferris DP. 2015. Isolating gait-related movement artifacts in electroencephalography during human walking. J Neural Eng. 12:046022.

la Fougère C, Zwergal A, Rominger A, Förster S, Fesl G, Dieterich M, Brandt T, Strupp M, Bartenstein P, Jahn K. 2010. Real versus imagined locomotion: a [18F]-FDG PET-fMRI comparison. Neuroimage. 50:1589–1598.

Leblond H, Ménard A, Gossard JP. 2001. Corticospinal control of locomotor pathways generating extensor activities in the cat. Exp Brain Res. 138:173–184.

Leuthardt EC, Schalk G, Wolpaw JR, Ojemann JG, Moran DW. 2004. A brain-computer interface using electrocorticographic signals in humans. J Neural Eng. 1:63–71.

Lisi G, Morimoto J. 2015. EEG single-trial detection of gait speed changes during treadmill walk. PLoS One. 10:e0125479.

Masdeu JC, Alampur U, Cavaliere R, Tavoulareas G. 1994. Astasia and gait failure with damage of the pontomesencephalic locomotor region. Ann Neurol. 35:619–621.

Miller KJ, Leuthardt EC, Schalk G, Rao RP, Anderson NR, Moran DW, Miller JW, Ojemann JG. 2007. Spectral changes in cortical surface potentials during motor movement. J Neurosci. 27:2424–2432.

Miyai I, Tanabe HC, Sase I, Eda H, Oda I, Konishi I, Tsunazawa Y, Suzuki T, Yanagida T, Kubota K. 2001. Cortical mapping of gait in humans: a near-infrared spectroscopic topography study. Neuroimage. 14:1186–1192.

Mori S. 1987. Integration of posture and locomotion in acute decerebrate cats and in awake, freely moving cats. Prog Neurobiol. 28:161–195.

Nathan PW. 1994. Effects on movement of surgical incisions into the human spinal cord. Brain. 117:337–346.

Niedermeyer E, da Silva FL. 2005. Electroencephalography: basic principles, clinical applications, and related fields. 5th ed. Philadelphia (PA): Lippincott Williams & Wilkins.

Nielsen JB. 2003. How we walk: central control of muscle activity during human walking. Neuroscientist. 9:195–204.

Pearson KG, Rossignol S. 1991. Fictive motor patterns in chronic spinal cats. J Neurophysiol. 66:1874–1887.

Penfield W, Rasmussen T. 1950. The cerebral cortex of man; a clinical study of localization of function. New York (NY): Macmillan.

Perry JB. 2010. Gait analysis: normal and pathological function. 2nd ed. Thorofare (NJ): Slack Incorporated.

Petersen NT, Butler JE, Marchand-Pauvert V, Fisher R, Ledebt A, Pyndt HS, Hansen NL, Nielsen JB. 2001. Suppression of EMG activity by transcranial magnetic stimulation in human subjects during walking. J Physiol. 537:651–656.

Petersen TH, Willerslev-Olsen M, Conway BA, Nielsen JB. 2012. The motor cortex drives the muscles during walking in human subjects. J Physiol. 590:2443–2452.

Pfurtscheller G, Graimann B, Huggins JE, Levine SP, Schuh LA. 2003. Spatiotemporal patterns of beta desynchronization and gamma synchronization in corticographic data during self-paced movement. Clin Neurophysiol. 114:1226–1236.

Prilutsky BI, Sirota MG, Gregor RJ, Beloozerova IN. 2005. Quantification of motor cortex activity and full-body biomechanics during unconstrained locomotion. J Neurophysiol. 94:2959–2969.

Raethjen J, Govindan RB, Binder S, Zeuner KE, Deuschl G, Stolze H. 2008. Cortical representation of rhythmic foot movements. Brain Res. 1236:79–84.

Rao RP, Scherer R. 2010. Statistical pattern recognition and machine learning in brain-computer interfaces. In: Oweiss KG, editor. Statistical signal processing for neuroscience and neurotechnology. Burlington (MA): Academic Press. p. 335–368.

Rossignol S, Dubuc R, Gossard JP. 2006. Dynamic sensorimotor interactions in locomotion. Physiol Rev. 86:89–154.

Ruescher J, Iljina O, Altenmüller DM, Aertsen A, Schulze-Bonhage A, Ball T. 2013. Somatotopic mapping of natural upper- and lower-extremity movements and speech production with high gamma electrocorticography. Neuroimage. 81: 164–177.

Schalk G, Leuthardt EC. 2011. Brain-computer interfaces using electrocorticographic signals. IEEE Rev Biomed Eng. 4: 140–154.

Schubert M, Curt A, Jensen L, Dietz V. 1997. Corticospinal input in human gait: modulation of magnetically evoked motor responses. Exp Brain Res. 115:234–246.

Seeber M, Scherer R, Wagner J, Solis-Escalante T, Müeller-Putz GR. 2014. EEG beta suppression and low gamma modulation are different elements of human upright walking. Front Hum Neurosci. 8:485.

Seeber M, Scherer R, Wagner J, Solis-Escalante T, Müeller-Putz GR. 2015. High and low gamma EEG oscillations in central

sensorimotor areas are conversely modulated during the human gait cycle. Neuroimage. 112:318–326.

Sinkjær T, Andersen JB, Ladouceur M, Christensen LO, Nielsen JB. 2000. Major role for sensory feedback in soleus EMG activity in the stance phase of walking in man. J Physiol. 523:817–827.

van Wijk B, Beek PJ, Daffertshofer A. 2012. Neural synchrony within the motor system: what have we learned so far? Front Hum Neurosci. 6:252.

Vilensky JA. 1987. Locomotor behavior and control in human and non-human primates: comparisons with cats and dogs. Neurosci Biobehav Rev. 11:263–274.

Vilensky JA, O'Connor BL. 1998. Stepping in nonhuman primates with a complete spinal cord transection: old and new data, and implications for humans. Ann N Y Acad Sci. 860:528–530.

Wang PT, King CE, Do AH, Nenadic Z. 2011. A durable, low-cost electrogoniometer for dynamic measurement of joint trajectories. Med Eng Phys. 33:546–552.

Wang PT, King CE, Schombs A, Lin JJ, Sazgar M, Hsu FP, Shaw SJ, Millett DE, Liu CY, Chui LA, et al. 2013a. Electrocorticogram encoding of upper extremity movement trajectories. Proc. 6th Int IEEE/EMBS Conf. Neural Eng. p. 1429–1432.

Wang W, Collinger JL, Degenhart AD, Tyler-Kabara EC, Schwartz AB, Moran DW, Weber DJ, Wodlinger B, Vinjamuri RK, Ashmore

RC, et al. 2013b. An electrocorticographic brain interface in an individual with tetraplegia. PLoS One. 8:e55344.

Wang PT, King CE, McCrimmon CM, Lin JJ, Sazgar M, Hsu FP, Shaw SJ, Millet DE, Chui LA, Liu CY, et al. 2016. Comparison of decoding resolution of standard and high-density electrocorticogram electrodes. J Neural Eng. 13:026016.

Whelan PJ. 1996. Control of locomotion in the decerebrate cat. Prog Neurobiol. 49:481–515.

Whitham EM, Pope KJ, Fitzgibbon SP, Lewis T, Clark CR, Loveless S, Broberg M, Wallace A, DeLosAngeles D, Lillie P, et al. 2007. Scalp electrical recording during paralysis: quantitative evidence that EEG frequencies above 20 Hz are contaminated by EMG. Clin Neurophysiol. 118:1877–1888.

Wieser M, Haefeli J, Bütler L, Jäncke L, Riener R, Koeneke S. 2010. Temporal and spatial patterns of cortical activation during assisted lower limb movement. Exp Brain Res. 203: 181–191.

Yanagisawa T, Hirata M, Saitoh Y, Kishima H, Matsushita K, Goto T, Fukuma R, Yokoi H, Kamitani Y, Yoshimine T. 2012. Electrocorticographic control of a prosthetic arm in paralyzed patients. Ann Neurol. 71:353–361.

Yogev-Seligmann G, Hausdorff JM, Giladi N. 2008. The role of executive function and attention in gait. Mov Disord. 23: 329–342.